Available online at www.sciencedirect.com
ScienceDirect
Magnetic Resonance Imaging 28 (2010) 1234 – 1243
MAGNETIC RESONANCE IMAGING

In contrast to BOLD: signal enhancement by extravascular water protons as an alternative mechanism of endogenous fMRI signal change

Chase R. Figley[a], Jordan K. Leitch[a], Patrick W. Stroman[a,b,c,*]

[a]Centre for Neuroscience Studies, Queen's University, Kingston, Ontario, Canada K7L 3N6
[b]Department of Diagnostic Radiology, Queen's University, Kingston, Ontario, Canada K7L 3N6
[c]Department of Physics, Queen's University, Kingston, Ontario, Canada K7L 3N6

Received 7 October 2009; revised 23 December 2009; accepted 8 January 2010

Abstract

Despite the popularity and widespread application of functional magnetic resonance imaging (fMRI) in recent years, the physiological bases of signal change are not yet fully understood. Blood oxygen level-dependant (BOLD) contrast — attributed to local changes in blood flow and oxygenation, and therefore magnetic susceptibility — has become the most prevalent means of functional neuroimaging. However, at short echo times, spin-echo sequences show considerable deviations from the BOLD model, implying a second, non-BOLD component of signal change. This has been dubbed "signal enhancement by extravascular water protons" (SEEP) and is proposed to result from proton-density changes associated with cellular swelling. Given that such changes are independent of magnetic susceptibility, SEEP may offer new and improved opportunities for carrying out fMRI in regions with close proximity to air–tissue and/or bone–tissue interfaces (e.g., the prefrontal cortex and spinal cord), as well as regions close to large blood vessels, which may not be ideally suited for BOLD imaging. However, because of the interdisciplinary nature of the literature, there has yet to be a thorough synthesis, tying together the various and sometimes disparate aspects of SEEP theory. As such, we aim to provide a concise yet comprehensive overview of SEEP, including recent and compelling evidence for its validity, its current applications and its future relevance to the rapidly expanding field of functional neuroimaging. Before presenting the evidence for a non-BOLD component of endogenous functional contrast, and to enable a more critical review for the nonexpert reader, we begin by reviewing the fundamental principles underlying BOLD theory.

Keywords: Astrocytes; BOLD; Brain; Cell swelling; Contrast mechanisms; fMRI; Proton-density; SEEP; Spinal cord

1. Introduction

Functional magnetic resonance imaging (fMRI) has gained widespread popularity throughout both scientific and popular media because of its ability to precisely and noninvasively map central nervous system (CNS) function. The ability to visualize the brain at work has already allowed researchers to study the neural correlates of sensation, perception, planning and action, and may be used in the foreseeable future to assist clinical diagnosis and surgical planning for a number of psychiatric and neurological disorders [1–4]. However, despite its extensive usage, the physiological mechanisms underlying fMRI are not yet fully understood [5,6].

Because of its speed, sensitivity and well-characterized response function, "blood oxygen level-dependant" (BOLD) fMRI has become the mainstay of functional neuroimaging. Although T_2^*-weighted gradient-echo (GE) pulse sequences with echo-planar imaging readouts (i.e., GE-EPI) provide optimal susceptibility-weighted contrast, BOLD responses can also be measured with T_2-weighted spin-echo (SE) sequences, but with ~3.5 times less sensitivity at a given echo time (TE) and ~2 times less sensitivity at the optimal TEs for BOLD contrast (i.e., $TE \approx T_2^*$ and T_2, respectively) [7,8]. However, these T_2-weighted signal changes have been shown to deviate significantly from the accepted BOLD model, exhibiting little-to-no signal reduction in spinal cord fMRI between GE and SE methods, and demonstrating a reduced dependence on TE, particularly at very short TEs

* Corresponding author. Departments of Diagnostic Radiology and Physics, c/o Centre for Neuroscience Studies, Queen's University, Kingston, Ontario, Canada K7L 3N6. Tel.: +1 613 533 3245; fax: +1 613 533 6840.
E-mail address: stromanp@post.queensu.ca (P.W. Stroman).

0730-725X/$ – see front matter © 2010 Elsevier Inc. All rights reserved.
doi:10.1016/j.mri.2010.01.005

[9–11]. These findings have led to the proposition of a second, non-BOLD component of endogenous signal change based on regional proton-density (PD) changes. This effect is called "signal enhancement by extravascular water protons" (SEEP) and has been attributed to increased tissue water content (primarily from cellular swelling) in regions of neuronal activity [11,12].

The ability to reliably detect SEEP with PD-weighted SE sequences has a number of potential advantages over traditional GE-EPI fMRI sequences. For one, this activity-dependent cell swelling may constitute a more direct measure of neural activity and is likely to be better spatially localized compared to hemodynamic changes that are dispersed throughout the adjacent venules and draining veins. Moreover, while susceptibility-weighted fMRI research is moving toward higher magnetic fields (now 7 T and beyond), functional contrast based on PD-weighted signal changes is largely field independent, aside from the incremental increase in image signal intensity at higher magnetic fields. Thus, using SEEP, fMRI has been done successfully at field strengths as low as 0.2 T [13–16]. Finally, because proton-density changes can be detected with SE sequences, image artifacts can be drastically reduced (compared to susceptibility-weighted images) in regions proximal to air–tissue and bone–tissue interfaces, including the spinal cord (Fig. 1; in close proximity to the lungs, vertebrae and intervertebral disks), as well as the prefrontal cortex and temporal lobes (near the sinuses and auditory canals).

However, despite its demonstrated utility for certain applications, the concept of SEEP has been met with some resistance and has yet to gain broad acceptance within the fMRI community. Recently, a number of approaches have validated SEEP as a non-BOLD component of functional signal change and a sensitive means of detecting neural function. Here, we aim to present and review the underlying principles of SEEP and critically examine the processes through which it has been validated. Finally, we present some recent applications of SEEP and suggest future directions for its utilization in functional neuroimaging.

With advances in fMRI methods and hardware, both temporal and spatial resolution are continually improving, allowing researchers to probe, with increasing detail, the complexities and intricacies of the brain and spinal cord. To date, fMRI has been used to study human brain and spinal cord function in healthy and pathological states [1–4,18], and has even been implemented to study brain function in nonhuman primates [19–21]. However, despite the myriad experimental conditions, the vast majority of contemporary fMRI studies have relied on BOLD signal changes. In fact, until recently, the existence of SEEP has been contested by claims that it may, in reality, not be independent of blood oxygen-related contributions [22,23]. Therefore, before discussing the SEEP effect in detail, we will briefly review the underlying theory of BOLD changes (for detailed reviews, see Raichle [24] and Logothetis [6,25,26]).

2. A bit about BOLD

The essence of BOLD fMRI, first described by Ogawa et al. [27–29], is an activity-dependent metabolic and hemodynamic response that affects the supply and relative

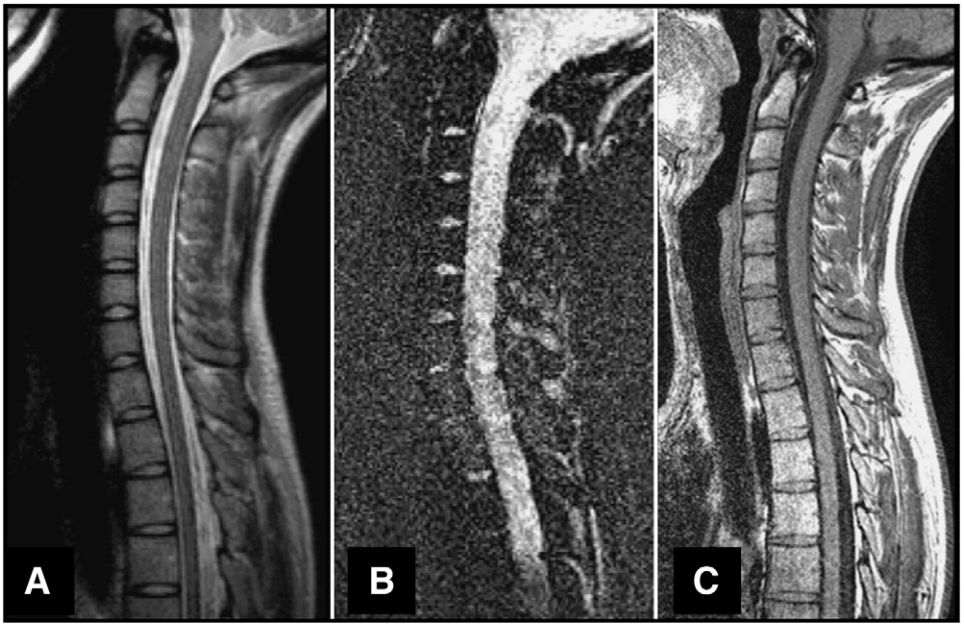

Fig. 1. Sagittal images of the spinal cord acquired with (A) PD-weighted half-Fourier acquisition single-shot turbo spin-echo (HASTE); (B) T_2*-weighted nine-shot GE, echo-planar imaging (GE-EPI); and (C) T_1-weighted turbo spin-echo (TSE) sequences. Even short readouts from a nine-shot GE-EPI do not eliminate susceptibility artifacts from the surrounding vertebrae and intervertebral discs. (Figure reproduced with permission from Bouwman et al. [17].)

proportion of oxygenated blood in regions of neural activity. Although Ogawa et al. [27–29] were the first to observe these changes with MRI, the link between brain activity, increased cerebral metabolic rate of oxygen (CMR_{O_2}) and elevated cerebral blood flow (CBF) had already been established in earlier positron emission tomography (PET) studies [30]. However, unlike PET, BOLD fMRI depends on the endogenous contrast resulting from the relative concentrations of oxyhemoglobin (Hb) and deoxyhemoglobin (dHb), which affects the T_2 and T_2^* relaxation times in the capillary beds, downstream venules and draining veins [31,32]. Of course, determining the physiological basis of these changes and understanding the relationship between hemodynamic and neuronal activity are of great importance, and much work has been done to elucidate this mechanism.

In the mid-1930s, Pauling and Coryell [33] characterized the chemical structure and magnetic properties of Hb and a number of its derivatives, determining that Hb is diamagnetic, whereas dHb is strongly paramagnetic. This disparity in magnetic susceptibility (between Hb and dHb) changes the tissue transverse relaxation rate (ΔR_2 or ΔR_2^*) such that $\Delta R \propto [\mathrm{dHb}]^{\beta}$, where ΔR is either ΔR_2 or ΔR_2^*, [dHb] is the concentration of dHb and β is an empirically determined parameter with a value between 1 and 2 [34,35]. Thus, the MR signal depends on the oxygen saturation of the blood, leading to blood oxygen-induced signal fluctuations proportional to the local ratio of CMR_{O_2}/CBF, known as the oxygen extraction fraction (OEF) [29,36,37].

The higher magnetic susceptibility of dHb reduces phase coherence, thereby lowering T_2- and T_2^*-weighted signals, so that the fractional signal change ($\Delta S/S$) is proportional to ΔR and roughly linear with TE for small BOLD changes (i.e., $\Delta S/S \ll 1$):

$$\Delta S / S \approx -\mathrm{TE}(\Delta R) \tag{1}$$

where, again, ΔR is ΔR_2 or ΔR_2^* (for SE or GE images, respectively), S is the baseline signal intensity and ΔS is the amount of signal change upon neuronal activation/deactivation [7]. Moreover, the change in transverse relaxation rate between two conditions, at time=0 (baseline) and time=t, can be related to the OEF changes, such that:

$$\Delta R \propto f_v(t)\left(\frac{\mathrm{CMR}_{O_2}(t)}{\mathrm{CBF}(t)}\right)^{\beta} - f_v(0)\left(\frac{\mathrm{CMR}_{O_2}(0)}{\mathrm{CBF}(0)}\right)^{\beta} \tag{2}$$

where f_v is the blood volume fraction [34].

In general, lowering the OEF serves to increase the BOLD signal and vice versa. Therefore, while elevated neural activity disproportionately increases blood flow, a lag between increased metabolic demand and oxygen delivery may result in a brief "initial dip" in BOLD signal [38–40]. After a few seconds, however, blood delivery supersedes the elevation in oxygen utilization, peaking approximately 5–8 s after the stimulus, depending on the task and brain region [41]. The corollary therefore is that regions of neural activity and the downstream blood volumes exhibit increased signal upon activation, due to an overabundant supply of Hb and reduced [dHb]. BOLD effects are therefore, by definition, due to hemodynamic changes that correspond with changes in neural input and local processing (i.e., synaptic activity) of neurons in a given region [42].

To optimize BOLD sensitivity, T_2- and T_2^*-weighted pulse sequences can be made highly sensitive to magnetic susceptibility changes, but this inherent sensitivity to magnetic susceptibility differences can also cause artifacts and signal dropout near air–tissue and bone–tissue interfaces (Fig. 1). Therefore, to investigate functional changes in the spinal cord (surrounded by vertebrae and intervertebral discs) and regions of the prefrontal cortex or temporal lobes in close proximity to the nasal sinuses or auditory canals, SEEP contrast may offer an important alternative to conventional BOLD fMRI methods.

3. Deviations from the BOLD model and early indications of SEEP

The first evidence for SEEP was obtained from a pair of studies trying to prove the existence of BOLD effects in the spinal cord, and although the first study [43] succeeded in showing that spinal fMRI was possible, the measured signal changes were abnormally large (approximately 7%) for BOLD, which is typically on the order of a few percent at 3 T. Thus, the second study [44] set out to compare the magnitude of the changes for SE and GE imaging methods. As described above, BOLD changes should depend on TE and changes in either T_2 or T_2^* relaxation rates (Eq. (1)), assuming a single relaxation environment and a constant proton density [45]. Moreover, because ΔR_2^* is greater than ΔR_2, GE methods should produce ~3.5 times larger BOLD signal changes than SE methods at a fixed TE [8]. However, the comparison between fMRI data acquired at the same TE in the spinal cord was not consistent with these predictions [44], demonstrating signal changes that were as large, or larger in SE images, as in the corresponding GE images (Fig. 2).

Subsequent studies confirmed that the same effects are also manifest in the spinal cord at 1.5 T [9] and in the brain at both 1.5 and 3 T [10] across a range of TEs. Here, both GE and SE methods exhibited a linear dependence on TE, with the measured T_2^* and T_2 relaxation rates (i.e., the slopes of these lines) corresponding to previous reports. As expected, the T_2^*-weighted signal extrapolated approximately to zero at TE=0 ms, whereas the SE data extrapolated to a positive value, predicting signal changes of approximately 1.0% in the brain and 2.5% in the spinal cord at TE=0 ms. Because the linear dependence on TE is consistent with BOLD effects, but the nonzero intercept is not, these data support the idea that SE sequences are sensitive to BOLD effects as well as an underlying mechanism that is independent of T_2 changes.

To better understand these results, SE fMRI data of the spinal cord were acquired at 1.5 T at a number of TEs between 11 ms (the lower limit of the scanner) and 66 ms [11]. As seen

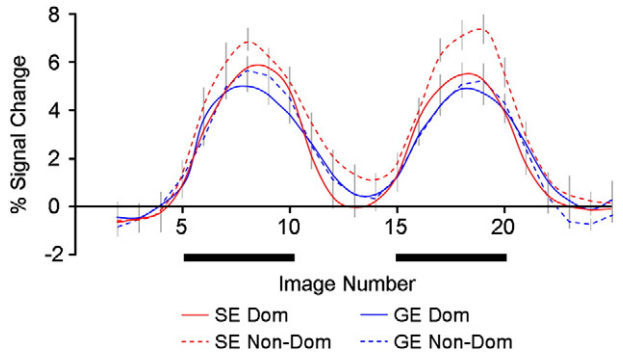

Fig. 2. Average fMRI signal time courses measured in the cervical spinal cord during a motor task (thick black bars) involving the dominant (solid lines) or nondominant hand (dashed lines). MR images were acquired with SE-EPI (red lines) and GE-EPI sequences (blue lines). Detecting larger signal changes with SE vs. GE pulse sequences is contrary to the BOLD model and the known relation between T_2 and T_2* relaxation rates. (Figure modified with permission from Stroman and Ryner [44].)

in Fig. 3, these results show that the signal changes deviate from zero as TE approaches zero and that this relationship is nonlinear, with a measured 3.3% signal change at a TE of only 11 ms. With the use of a two-component model to fit the data, allowing both relaxation time and proton-density changes, one relaxation component was found to be consistent with BOLD changes at 1.5 T, having a constant proton density and T_2 increasing from 172±9 ms (baseline) to 200±13 ms during thermal stimulation. The second component had a constant T_2 value of 71±21 ms, consistent with other reports of spinal cord relaxation at 1.5 T [46] and 3 T [47], but with a proton-density increase of 5.6±0.2% during stimulation. Because the model suggested that the measured signals included a BOLD component, as well as an increase in proton density in a compartment with a T_2 value too short to be attributed to blood, the second mechanism was called "signal enhancement by extravascular water protons" or "SEEP."

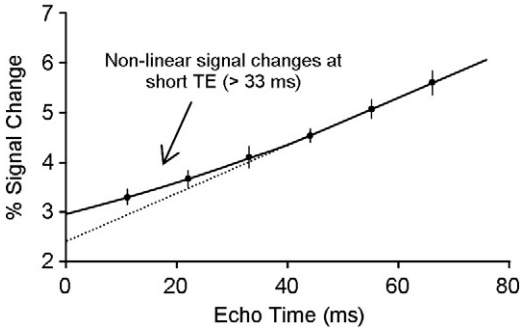

Fig. 3. Turbo spin-echo spinal fMRI data at 1.5 T are plotted (mean±S.E.M.; across 15 subjects) as a function of TE. The dashed and solid lines illustrate linear and nonlinear fits, respectively. The linear relation $\Delta S/S$=0.047 TE+2.4 (R^2=0.998) extrapolates to ~2.5% signal change at TE=0 ms and holds only for TE ≥33 ms. The nonlinear model predicts a signal change closer to ~3%. (Figure reproduced with permission from Stroman et al. [11].)

Further evidence for SEEP has been observed in brain fMRI studies at 0.2, 0.35, 1.5 and 3 T [13,15,48,49] and in spinal fMRI studies at 0.2 T [16,50,51]. Because susceptibility weighting is reduced at low field, BOLD contributions at 0.2 T are thought to be negligible. These experiments also demonstrate consistent features across a range of field strengths, with fractional signal changes of approximately 2% in the brain. Even as low as 0.2 T, fMRI studies during a motor task showed robust signal changes of 2.1±0.2% and 2.3±0.1% with the right and left hands, and 1.7±0.1% and 2.0±0.2% during thermal stimulation (Fig. 4). At 1.5 and 3 T, the signal changes were observed to be 1.9±0.2% and 1.9±0.3%, respectively, during a similar thermal stimulation paradigm. Given that BOLD effects exhibit substantial field-strength dependence [52], the consistency of these changes across field strengths supports a mechanism based on proton-density changes. Another consistent feature is that areas of activity observed with BOLD and SEEP fMRI are in close correspondence, but with little overlap, fitting together like puzzle pieces [10,48,49].

The most recent and most direct observation of the SEEP contrast mechanism was obtained with fMRI studies of rat cortical tissue slices [12]. This study used a predominantly PD-weighted turbo spin-echo (TSE) sequence, with similar parameters used for SEEP fMRI, and light-transmittance (LT) microscopy [53,54] to measure proton-density changes induced by neural activity and osmotic challenges. Time-series MRI data acquired from living, superfused brain slices revealed that the signal intensity reversibly increased with potassium-evoked neu-

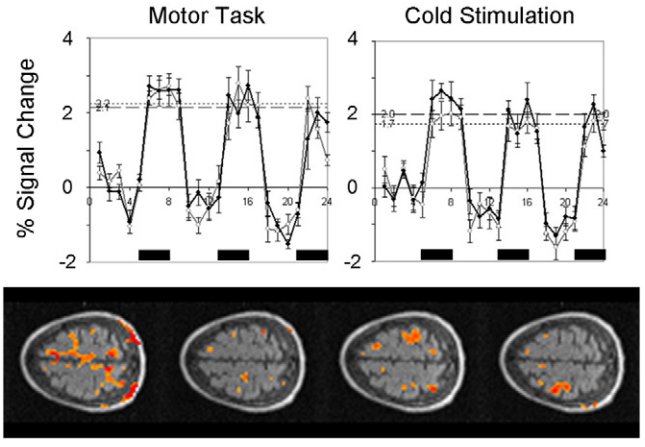

Fig. 4. Robust signal intensity changes observed with proton density-weighted (PD-weighted) fMRI at 0.2 T. (Top) While susceptibility-weighted functional contrast is not expected with these imaging parameters and at such low field strengths, right-hand (RH) and left-hand (LH) motor tasks (black bars) elicited 2.1±0.2% and 2.3±0.1% signal changes (mean±S.E.M.), respectively, while thermal stimulation (black bars) produced signal changes of 1.7±0.1% and 2.0±0.2%. These values overlap with signal changes at 3 T under similar conditions, further implicating field-independent PD changes as the contrast mechanism. (Bottom) Regions of activity (T ≥2.80) during RH motor, LH motor, RH sensory and LH sensory tasks (from left to right) shown in radiological orientation. (Figures reproduced with permission from Stroman et al. 2003 [13].)

ronal depolarizations and, in separate experiments, osmotic challenge. These changes were observed in the absence of either blood-flow or blood-oxygen fluctuations and therefore cannot have any residual BOLD contributions, as previously argued [22,23]. The fact that LT signals changed over a similar time-course confirms that the MRI signals were in fact related to activity-induced cell swelling. Moreover, because the observed changes were reversible and ≥2%, they are thought to closely reflect nonpathological in vivo conditions. It should also be noted that this kind of activity-dependent tissue swelling is a well-known phenomenon that has been previously demonstrated using a number of physiological techniques including extracellular space measurements [55,56], increased light transmittance [53,57,58] and increased extracellular resistance [59]. Thus, studies of cell physiology, using methods other than MRI and predating fMRI, have shown that PD increases are expected to accompany increased neural activity.

4. Controversies surrounding water proton-density changes associated with functional magnetic resonance imaging

To date, the strongest argument against SEEP contrast comes from a study by Jochimsen et al. [23], in which the authors investigated fMRI signal changes with SE methods at 3 T, over a range of TEs (from 9 to 39 ms, as well as a BOLD "reference" dataset at 80 ms). Although they conclude that there is no significant contribution from proton-density changes, the analysis methods employed in this study relied heavily on several significant assumptions, each of which reduced the sensitivity of their data to non-BOLD effects. As it was not specified in the manuscript, it is implied that their analysis employed a model of the expected BOLD response, with the subsequent statistical thresholding and Bonferroni corrections designed to exclude changes which do not match the BOLD model. However, data from both the brain and spinal cord have consistently demonstrated that proton-density changes do not follow the same time course [11,48,49], with SEEP responses lagging BOLD responses by roughly 1–2 s and likely lacking a post-stimulus undershoot [49]. Moreover, because it has been shown that areas of SEEP activity are immediately adjacent to BOLD activations, but with little overlap [48], the use of a mask based on BOLD signal changes (from the dataset acquired at TE=80 ms) would have preferentially excluded areas of proton-density change. The results presented by Jochimsen et al. [23] with this particular analysis are therefore expected to demonstrate only the BOLD effect and do not refute the possibility of a proton-density change contribution to SE fMRI data.

One very interesting feature of their findings, however, was that even at a TE of 9 ms, an average of 65 active voxels were detected in the six volunteers studied [23], and even though ~9 of these voxels may have been false positives based on the statistical analysis, this implies that, on average, 56 of these voxels were likely true positives. With the reduced sensitivity to non-BOLD effects that was imposed by their analysis, the data presented remarkably still demonstrate activity in the visual cortex with SE data at TE=9 ms, where the BOLD effect is minute, with an average signal change of roughly 0.75% across the six subjects. The authors were able to eliminate these regions of activity by applying a Bonferroni correction based on ~1700 voxels, but the need to increase the statistical threshold to eliminate these regions confirms only that the observed signal changes did not match the expected BOLD model. Therefore, the authors convincingly demonstrate that this activity cannot be attributed to the BOLD effect, but the conclusion that these are false-positive results is only one of several possible explanations and does not rule out the possibility of non-BOLD changes such as SEEP.

5. Diffusion fMRI and corroborating evidence for activity-related cellular swelling

In contrast to freely diffusing water molecules which undergo random isotropic motion, water in cellular structures undergoes restricted diffusion. Thus, diffusion-weighted MRI [60] can serve as a surrogate marker for both tissue microstructure and neural function. With low diffusion sensitivity (i.e., low b values, on the order of a few hundred s/mm^2), it is generally accepted that increased apparent diffusion coefficients (ADC) result from increased capillary and vascular blood flow in regions of neural activity [61–64]. However, since flow velocities are not expected to change appreciably in large veins and arterial blood flow is turbulent, these ADC changes are thought to originate from small arterioles and capillaries, yielding higher spatial localization to neural activity than susceptibility-weighted fMRI [61].

Conversely, because passive diffusion processes are much slower than blood flow, it was initially proposed that high diffusion sensitivities (i.e., b values $\gg$1500 s/mm^2) should restrict signal changes to tissue volumes, while eliminating vascular contributions [65]. Le Bihan et al. [66] have proposed a model for these changes where the volume fractions of slow and fast diffusion compartments are shifted, with increased contributions from the slow diffusion pool as a result of transient cell swelling in active neural tissue (see Ref. [67] for a detailed explanation). Similar ADC decreases with high diffusion sensitivity have now been replicated in a number of studies [65–70], but the origin of these changes has been questioned, with other groups suggesting that the signals may contain vascular contributions [71,72]. Although SEEP and diffusion fMRI are measured with different parameters, recent evidence for SEEP may also validate cell swelling as the primary mechanism for high b-value diffusion fMRI.

While fMRI is not the most sensitive method for imaging neuronal activity in tissue slices, direct comparisons between SEEP fMRI and time-resolved LT microscopy have shown that cell swelling does occur with neural activity, and that these changes can be reliably detected with PD-weighted fMRI [12]. Since no blood was present in these tissue preparations, and because there is no vascular response in situ, this proves that cell swelling can occur independently of blood flow or blood oxygenation, and supports the theory of Le Bihan et al. [65–68] that high *b*-value diffusion fMRI signals reflect cellular, as opposed to vascular, changes. Recent reports that neurons lack water channels (called "aquaporins") further imply that this type of cellular swelling is likely to occur primarily in astrocytes, as opposed to neurons, under normal physiological conditions [53,73]. The preponderance of evidence therefore suggests that SEEP and diffusion fMRI share a common physiological mechanism, based predominantly on astrocyte swelling (and therefore increased proton density and tissue tortuosity), rather than on residual BOLD contributions or vascular effects near sites of neuronal activity (Fig. 5).

6. Advantages and applications of SEEP

6.1. Advantages and applications of SEEP at high field

As described above, SEEP effects can be measured with PD-weighted TSE (as opposed to susceptibility-weighted) imaging parameters and therefore offer an alternative to conventional BOLD imaging. Because TSE images are robust to artifacts resulting from poor field homogeneity, the most common application of SEEP, to date, has been to perform fMRI in the brainstem and spinal cord (see Leitch et al. in this issue for a comprehensive review). On the other hand, even multishot GE-EPI sequences with short readout times suffer from severe magnetic susceptibility artifacts from the vertebrae and intervertebral disks (see Fig. 1), thereby limiting the use of GE-EPI for spinal fMRI.

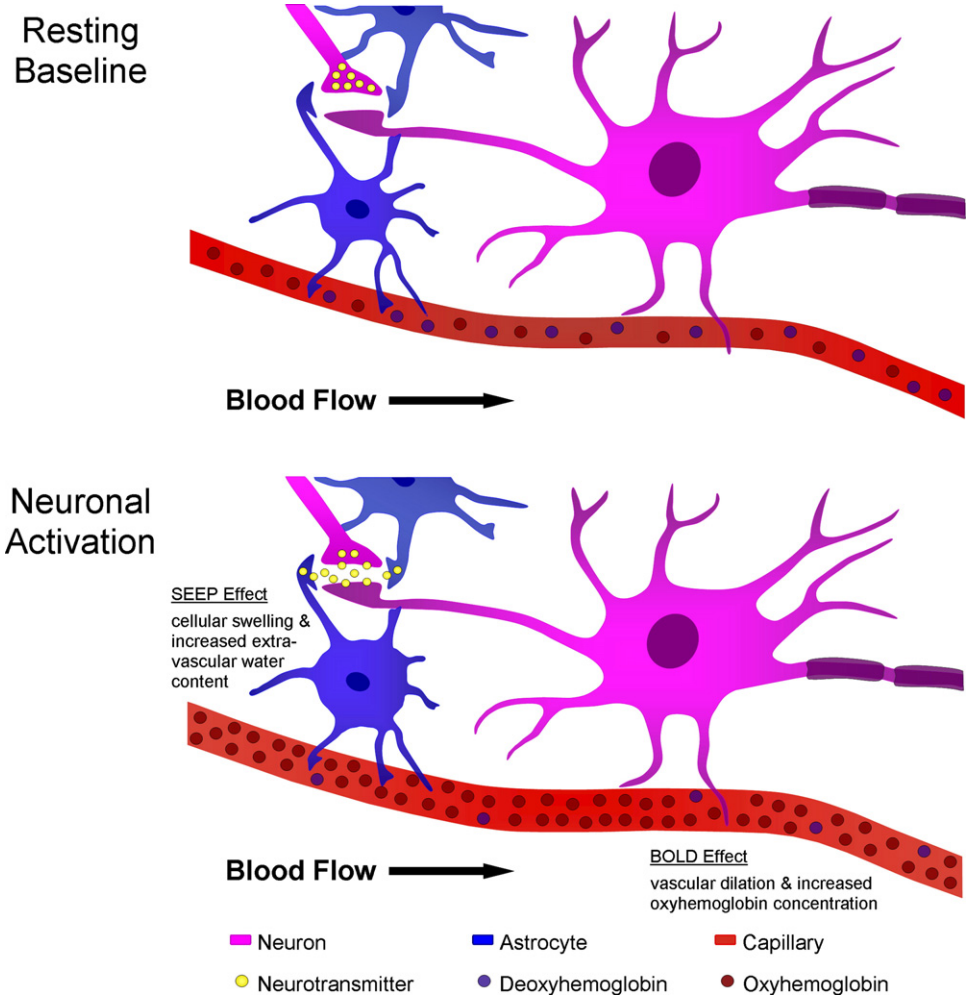

Fig. 5. Biophysical models of SEEP and BOLD effects. While both are indirect measures of neural activity, SEEP contrast is based on endogenous proton-density changes that are thought to result from astrocyte swelling and increased tissue water content in active neural tissue. On the other hand, hemodynamic effects such as BOLD contrast are sensitive to a cascade of physiological responses that change CBF, CMR_{O_2} and oxygen saturation in capillaries, venules and draining veins downstream from the sites of neuronal activity.

Although segmented GE-EPI acquisitions reduce spatial distortions and improve signal-to-noise ratios compared to single-shot GE-EPI methods, multishot acquisitions increase the effective TR (largely eliminating the gain in speed provided by EPI) and produce lower image quality compared to half-Fourier single-shot acquisition turbo spin-echo (HASTE) sequences (Fig. 1). Moreover, segmented acquisitions do not allow retrospective motion correction [74–76], since different phases of structured noise are coalesced into each image.

The relative insensitivity of SEEP methods to magnetic field distortions also provides significant benefits in certain clinical situations. For example, SEEP imaging has now been used to carry out fMRI in close proximity to metal fixation devices, which are routinely implanted into the vertebrae after spinal cord trauma (see Leitch et al. in this issue). Due to the combination of vertebrae, intervertebral disks and the metal implant, BOLD imaging (even with segmented acquisitions) would not be possible in this situation. Thus, SEEP offers an alternative to BOLD-sensitive fMRI techniques, which may expand the clinical utility of fMRI in cases where metal implants (e.g., dental braces, permanent metal retainers, maxillofacial screws and other surgical steels) are present.

The demonstrated ability to obtain fMRI data throughout the brainstem and spinal cord, even in the presence of implanted vertebral fixation devices, suggests that the SEEP method might also be effective for performing fMRI in other areas of poor field homogeneity such as the frontal and temporal lobes. Due to their close proximities to the sinuses and inner-ear structures, conventional GE-EPI BOLD fMRI parameters show considerable spatial distortions and signal dropout in regions of the anterior prefrontal cortex and lateral temporal lobes compared to TSE sequences [77,78]. Thus, even though SEEP contrast (to our knowledge) has not yet been applied in either frontal or temporal lobe fMRI studies, PD-weighted SE pulse sequences, similar to those used for spinal fMRI, are expected to provide distortion-free images with high signal- and contrast-to-noise ratios in these regions.

6.2. Advantages and applications of SEEP at low field

Although every MR image depends inherently on the local proton density, image contrast can also be made to depend on the different relaxation times (T_1, T_2 or T_2*) of various tissues. It is important to consider, however, that additional contrast based on tissue relaxation requires an inherent signal reduction because of decreased longitudinal (T_1) or transverse (T_2 or T_2*) magnetization. Therefore, another advantage of proton-density imaging is that it provides the highest signal-to-noise ratio of any endogenous MRI contrast mechanism. Moreover, proton-density changes are relatively insensitive to changes in magnetic field strength [79,80], whereas transverse relaxation changes (ΔT_2 and ΔT_2*) exhibit significant field dependence [81], providing better functional contrast in BOLD-based fMRI methods at higher magnetic fields [52].

By relying on changes in proton density, fMRI based on SEEP contrast has been performed at field strengths as low as 0.2 T [13,14,16] and 0.35 T [15,82], where BOLD imaging would not be possible. The ability to obtain fMRI data at such low magnetic fields may be of little advantage for most modern hospitals and research centers, but for various reasons, this may still be beneficial. For instance, many vendors are now/still marketing MRI systems under 1.0 T that are based on permanent magnets (for lower cost and easier maintenance) and/or open designs (to reduce claustrophobia, accommodate large patients and allow MRI-guided interventions). While these systems suffer the same signal-to-noise reductions encountered for any low-field imaging, SEEP contrast, based on proton-density changes, presents a viable option for centers with these systems to perform fMRI.

6.3. Evidence for better spatial localization

By measuring cell swelling, as opposed to vascular changes, SEEP fMRI is expected to provide better localization than BOLD fMRI to the actual sites of neuronal activity. BOLD fMRI can reveal relatively large areas of apparent activation because of the diffuse nature of venules and veins draining blood from the active regions. This phenomenon has been directly investigated by mapping both SEEP and BOLD fMRI responses within the same subjects and during the same visual and/or motor tasks [10,48,49]. In these studies, both SEEP and BOLD contrasts demonstrated robust activations throughout the expected regions, but depending on the type of functional contrast, the areas of activity were consistently observed to be directly adjacent to each other, with little overlap. These empirical findings both support the different neurophysiological underpinnings of SEEP and BOLD (Fig. 5), and demonstrate that SEEP signal changes are more localized to the actual sites of neuronal activity compared to BOLD signal changes.

The ability to measure functional changes with greater spatial specificity has many important implications. For example, BOLD signal changes in the spinal cord are manifest within the draining veins along the periphery of the cord [83], whereas SEEP may provide more detailed information about the complex functional architecture within each spinal cord segment.

7. Limitations of SEEP contrast

It is important to point out that, although SEEP and BOLD measure different physiological parameters related to neuronal activity, these contrast mechanisms are not contradictory or mutually exclusive. The biophysical models for each are well documented, and it is now established that neural activity elicits both hemodynamic and cellular changes. Moreover, studies comparing SEEP

and BOLD contrasts have shown that the regions of signal change, regardless of imaging method, are in close enough proximity that conclusions drawn from either dataset are synonymous within the limitations of fMRI in general. Therefore, the choice of optimal contrast will be determined by the nature of the application and the experimental conditions, giving due consideration to the requisite trade-offs between image quality, spatial resolution, temporal resolution and statistical power. While SEEP has superior image quality and arguably better spatial resolution, BOLD imaging has significant advantages in terms of temporal resolution and statistical power.

The disadvantages of SEEP fMRI obtained with SE methods, and particularly with fast SE methods (i.e. non-EPI readout schemes), include higher energy deposition in tissues [specific absorption ratio (SAR)] and longer image acquisition times. Fast SE methods consist of a 90° excitation pulse followed by a train of 180° refocusing pulses, and the RF energy deposited in the tissues can therefore be two orders of magnitude higher than GE-EPI sequences. For safety reasons and because of SAR safety limits, this can impose severe limits on the number of slices that can be imaged in a given time interval.

Limits on the speed of SEEP fMRI are also imposed by the relatively long TRs and readout times inherent with PD-weighted fast SE imaging sequences. Even HASTE pulse sequences require repetition times (TRs) between 0.75 and 1 s per slice [17,18]. Therefore, to acquire data from a whole-brain volume (~90 mm in the smallest dimension) with 3-mm contiguous slices would require an effective TR somewhere between 22 and 30 s, which is impractical. On the other hand, GE-EPI sequences could acquire the same volume, with comparable resolution, in as little as 2 to 2.5 s, while advanced parallel imaging parameters such as PRESTO-SENSE are now able to achieve whole-brain temporal resolution in as little as 1 s [84]. Thus, there is a substantial tradeoff between temporal resolution and resilience to artifact when comparing SEEP- and single-shot BOLD-based acquisition methods. In addition, the use of GE-EPI and other fast imaging methods is required to perform rapid event-related fMRI over large regions of interest, while reliably identifying regions of neural activity [85–87].

As discussed above, the areas of activity detected with SEEP are more spatially localized and less diffuse than those detected with BOLD, and while this is generally advantageous, it can also be viewed as a disadvantage. Smaller areas of activity require higher resolution to avoid loss of sensitivity from spatial partial volume effects. Moreover, small and isolated regions of activity are vulnerable to motion because of temporal partial volume averaging, and while sophisticated post hoc modeling and analyses methods can improve the sensitivity of fMRI data, smaller regions remain more prone to motion-induced type II (false-negative) errors. Thus, in spite of the greater spatial localization of SEEP contrast, this can also present greater challenges for the detection of neuronal activity.

8. Concluding remarks

Perhaps the primary challenge for SEEP has been to bridge many disparate scientific disciplines, including imaging physics, neurophysiology, cell biology and systems/cognitive neuroscience. Because each of these disciplines comes with its own lexicon and common knowledgebase, we have tried to present, in one manuscript, a balanced review of the SEEP literature, laying out its physiological basis, its strengths and its weaknesses.

We are not suggesting that SEEP should or will replace BOLD contrast as the primary mechanism to noninvasively map the functional architecture of the CNS under most circumstances. The sensitivity and temporal resolution of GE-EPI parameters allow large volume coverage, short (<1 s) TRs and event-related study paradigms with high statistical power and reasonable scan times — and this makes it a powerful tool. However, because the SEEP contrast is based largely on proton-density changes, SE imaging methods can be used without EPI readouts to provide images that are relatively insensitive to magnetic field distortions. Therefore, SEEP is also a powerful mechanism of endogenous contrast that can be exploited to perform functional imaging at low field strengths, in clinical populations with metal implants and in CNS regions throughout the brain, brainstem and spinal cord that are not amenable to BOLD imaging.

Acknowledgments

We gratefully acknowledge the funding support provided by the International Spinal Research Trust (UK), the Canada Research Chairs Program, the National Sciences and Engineering Research Council of Canada, the Craig H. Nielsen Foundation, the Canadian Institutes of Health Research Canada Graduate Scholarships Program, and the Queen's University Faculty of Health Sciences Harry Botterell Foundation. We are also grateful to Teresa McAdam and Randi Beazer for their valuable input and to Sharon David for technical support.

References

[1] Jezzard P, Buxton RB. The clinical potential of functional magnetic resonance imaging. J Magn Reson Imaging 2006;23(6):787–93.
[2] Matthews PM, Honey GD, Bullmore ET. Applications of fMRI in translational medicine and clinical practice. Nat Rev Neurosci 2006;7(9):732–44.
[3] Detre JA. Clinical applicability of functional MRI. J Magn Reson Imaging 2006;23(6):808–15.
[4] Owen AM, Coleman MR. Functional neuroimaging of the vegetative state. Nat Rev Neurosci 2008;9(3):235–43.
[5] Logothetis NK. The ins and outs of fMRI signals. Nat Neurosci 2007;10(10):1230–2.
[6] Logothetis NK. What we can do and what we cannot do with fMRI. Nature 2008;453(7197):869–78.
[7] Menon RS, Ogawa S, Tank DW, Ugurbil K. 4 Tesla gradient recalled echo characteristics of photic stimulation-induced signal changes in the human primary visual cortex. Magn Reson Med 1993;30(3):380–6.
[8] Bandettini PA, Wong EC, Jesmanowicz A, Hinks RS, Hyde JS. Spin-echo and gradient-echo EPI of human brain activation using BOLD

contrast: a comparative study at 1.5 T. NMR Biomed 1994;7(1-2): 12–20.
[9] Stroman PW, Krause V, Malisza KL, Frankenstein UN, Tomanek B. Characterization of contrast changes in functional MRI of the human spinal cord at 1.5 T. Magn Reson Imaging 2001;19(6):833–8.
[10] Stroman PW, Krause V, Frankenstein UN, Malisza KL, Tomanek B. Spin-echo versus gradient-echo fMRI with short echo times. Magn Reson Imaging 2001;19(6):827–31.
[11] Stroman PW, Krause V, Malisza KL, Frankenstein UN, Tomanek B. Extravascular proton-density changes as a non-BOLD component of contrast in fMRI of the human spinal cord. Magn Reson Med 2002;48 (1):122–7.
[12] Stroman PW, Lee AS, Pitchers KK, Andrew RD. Magnetic resonance imaging of neuronal and glial swelling as an indicator of function in cerebral tissue slices. Magn Reson Med 2008;59(4):700–6.
[13] Stroman PW, Malisza KL, Onu M. Functional magnetic resonance imaging at 0.2 tesla. NeuroImage 2003;20(2):1210–4.
[14] Li G, Ng MC, Wong KK, Luk KD, Yang ES. Spinal effects of acupuncture stimulation assessed by proton density-weighted functional magnetic resonance imaging at 0.2 T. Magn Reson Imaging 2005;23(10):995–9.
[15] Yang P, Wang J, Chao Y, Lu G, Shi J. Proton density-weighted functional magnetic resonance imaging at 0.35 tesla. The 2nd International Conference on Bioinformatics and Biomedical Engineering 2008:2260–3.
[16] Ng MC, Wong KK, Li G, Lai S, Yang ES, Hu Y, et al. Proton-density-weighted spinal fMRI with sensorimotor stimulation at 0.2 T. NeuroImage 2006;29(3):995–9.
[17] Bouwman CJ, Wilmink JT, Mess WH, Backes WH. Spinal cord functional MRI at 3 T: gradient echo echo-planar imaging versus turbo spin echo. NeuroImage 2008;43(2):288–96.
[18] Stroman PW. Magnetic resonance imaging of neuronal function in the spinal cord: spinal FMRI. Clin Med Res 2005;3(3):146–56.
[19] Zhang Z, Andersen AH, Avison MJ, Gerhardt GA, Gash DM. Functional MRI of apomorphine activation of the basal ganglia in awake rhesus monkeys. Brain Res 2000;852(2):290–6.
[20] Logothetis NK, Guggenberger H, Peled S, Pauls J. Functional imaging of the monkey brain. Nat Neurosci 1999;2(6):555–62.
[21] Disbrow E, Roberts TP, Slutsky D, Krubitzer L. The use of fMRI for determining the topographic organization of cortical fields in human and nonhuman primates. Brain Res 1999;829(1-2):167–73.
[22] Jin T, Wang P, Tasker M, Zhao F, Kim SG. Source of nonlinearity in echo-time-dependent BOLD fMRI. Magn Reson Med 2006;55(6): 1281–90.
[23] Jochimsen TH, Norris DG, Moller HE. Is there a change in water proton density associated with functional magnetic resonance imaging? Magn Reson Med 2005;53(2):470–3.
[24] Raichle ME. Behind the scenes of functional brain imaging: a historical and physiological perspective. Proc Natl Acad Sci U S A 1998;95(3): 765–72.
[25] Logothetis NK. The underpinnings of the BOLD functional magnetic resonance imaging signal. J Neurosci 2003;23(10):3963–71.
[26] Logothetis NK, Pfeuffer J. On the nature of the BOLD fMRI contrast mechanism. Magn Reson Imaging 2004;22(10):1517–31.
[27] Ogawa S, Lee TM, Nayak AS, Glynn P. Oxygenation-sensitive contrast in magnetic resonance image of rodent brain at high magnetic fields. Magn Reson Med 1990;14(1):68–78.
[28] Ogawa S, Lee TM, Kay AR, Tank DW. Brain magnetic resonance imaging with contrast dependent on blood oxygenation. Proc Natl Acad Sci U S A 1990;87(24):9868–72.
[29] Ogawa S, Tank DW, Menon R, Ellermann JM, Kim SG, Merkle H, et al. Intrinsic signal changes accompanying sensory stimulation: functional brain mapping with magnetic resonance imaging. Proc Natl Acad Sci U S A 1992;89(13):5951–5.
[30] Fox PT, Raichle ME. Focal physiological uncoupling of cerebral blood flow and oxidative metabolism during somatosensory stimulation in human subjects. Proc Natl Acad Sci U S A 1986;83(4):1140–4.
[31] Buxton RB, Frank LR. A model for the coupling between cerebral blood flow and oxygen metabolism during neural stimulation. J Cereb Blood Flow Metab 1997;17(1):64–72.
[32] Buxton RB, Wong EC, Frank LR. Dynamics of blood flow and oxygenation changes during brain activation: the balloon model. Magn Reson Med 1998;39(6):855–64.
[33] Pauling L, Coryell CD. The magnetic properties and structure of hemoglobin, oxyhemoglobin and carbonmonoxyhemoglobin. Proc Natl Acad Sci U S A 1936;22(4):210–6.
[34] Davis TL, Kwong KK, Weisskoff RM, Rosen BR. Calibrated functional MRI: mapping the dynamics of oxidative metabolism. Proc Natl Acad Sci U S A 1998;95(4):1834–9.
[35] Buxton RB, Uludag K, Dubowitz DJ, Liu TT. Modeling the hemodynamic response to brain activation. NeuroImage 2004;23 (Suppl 1):S220–33.
[36] Bandettini PA, Wong EC, Hinks RS, Tikofsky RS, Hyde JS. Time course EPI of human brain function during task activation. Magn Reson Med 1992;25(2):390–7.
[37] Turner R, Le BD, Moonen CT, Despres D, Frank J. Echo-planar time course MRI of cat brain oxygenation changes. Magn Reson Med 1991; 22(1):159–66.
[38] Ernst T, Hennig J. Observation of a fast response in functional MR. Magn Reson Med 1994;32(1):146–9.
[39] Buxton RB. The elusive initial dip. NeuroImage 2001;13(6 Pt 1): 953–8.
[40] Lindquist MA, Zhang CH, Glover G, Shepp L. Rapid three-dimensional functional magnetic resonance imaging of the initial negative BOLD response. J Magn Reson 2008;191(1):100–11.
[41] Handwerker DA, Ollinger JM, D'esposito M. Variation of BOLD hemodynamic responses across subjects and brain regions and their effects on statistical analyses. NeuroImage 2004;21(4):1639–51.
[42] Logothetis NK, Pauls J, Augath M, Trinath T, Oeltermann A. Neurophysiological investigation of the basis of the fMRI signal. Nature 2001;412(6843):150–7.
[43] Stroman PW, Nance PW, Ryner LN. BOLD MRI of the human cervical spinal cord at 3 tesla. Magn Reson Med 1999;42(3):571–6.
[44] Stroman PW, Ryner LN. Functional MRI of motor and sensory activation in the human spinal cord. Magn Reson Imaging 2001;19(1):27–32.
[45] Whittall KP, MacKay AL, Graeb DA, Nugent RA, Li DK, Paty DW. In vivo measurement of T2 distributions and water contents in normal human brain. Magn Reson Med 1997;37(1):34–43.
[46] Stanisz GJ, Odrobina EE, Pun J, Escaravage M, Graham SJ, Bronskill MJ, et al. T1, T2 relaxation and magnetization transfer in tissue at 3T. Magn Reson Med 2005;54(3):507–12.
[47] Smith SA, Edden RA, Farrell JA, Barker PB, Van Zijl PC. Measurement of T1 and T2 in the cervical spinal cord at 3 tesla. Magn Reson Med 2008;60(1):213–9.
[48] Stroman PW, Tomanek B, Krause V, Frankenstein UN, Malisza KL. Functional magnetic resonance imaging of the human brain based on signal enhancement by extravascular protons (SEEP fMRI). Magn Reson Med 2003;49(3):433–9.
[49] Stroman PW, Kornelsen J, Lawrence J, Malisza KL. Functional magnetic resonance imaging based on SEEP contrast: response function and anatomical specificity. Magn Reson Imaging 2005;23 (8):843–50.
[50] Ng MC, Wong KK, Li G, Ma QY, Yang ES, Hu Y, et al. Verification of proton density change in spinal cord fMRI. Proceedings of the Fourth IASTED International Conference on Visualization, Imaging, and Image Processing Sept 6–8, 2004, Marbella, Spain; 2004. p. 926–30.
[51] Wong KK, Ng MC, Hu Y, Luk DK, Ma QY, Yang ES. Functional MRI of the spinal cord at low field. Proceedings of the International Society for Magnetic Resonance in Medicine 12th Annual Meeting, Kyoto, Japan, May 15–21, 2004; 2004. poster 1534.
[52] Gati JS, Menon RS, Ugurbil K, Rutt BK. Experimental determination of the BOLD field strength dependence in vessels and tissue. Magn Reson Med 1997;38(2):296–302.

[53] Andrew RD, Jarvis CR, Obeidat AS. Potential sources of intrinsic optical signals imaged in live brain slices. Methods 1999;18(2): 185–96, 179.
[54] Andrew RD, Labron MW, Boehnke SE, Carnduff L, Kirov SA. Physiological evidence that pyramidal neurons lack functional water channels. Cereb Cortex 2007;17(4):787–802.
[55] Svoboda J, Sykova E. Extracellular space volume changes in the rat spinal cord produced by nerve stimulation and peripheral injury. Brain Res 1991;560(1-2):216–24.
[56] Krizaj D, Rice ME, Wardle RA, Nicholson C. Water compartmentalization and extracellular tortuosity after osmotic changes in cerebellum of *Trachemys scripta*. J Physiol 1996;492(Pt 3):887–96.
[57] MacVicar BA, Hochman D. Imaging of synaptically evoked intrinsic optical signals in hippocampal slices. Journal of Neuroscience 1991;11 (5):1458–69.
[58] Andrew RD, MacVicar BA. Imaging cell volume changes and neuronal excitation in the hippocampal slice. Neuroscience 1994;62 (2):371–83.
[59] Traynelis SF, Dingledine R. Role of extracellular-space in hyperosmotic suppression of potassium-induced electrographic seizures. Journal of Neurophysiology 1989;61(5):927–38.
[60] Le Bihan D, Breton E, Lallemand D, Grenier P, Cabanis E, Laval-Jeantet M. MR imaging of intravoxel incoherent motions: application to diffusion and perfusion in neurologic disorders. Radiology 1986;161 (2):401–7.
[61] Song AW, Woldorff MG, Gangstead S, Mangun GR, McCarthy G. Enhanced spatial localization of neuronal activation using simultaneous apparent-diffusion-coefficient and blood-oxygenation functional magnetic resonance imaging. NeuroImage 2002;17(2):742–50.
[62] Gangstead SL, Song AW. On the timing characteristics of the apparent diffusion coefficient contrast in fMRI. Magn Reson Med 2002;48(2): 385–8.
[63] Jin T, Zhao F, Kim SG. Sources of functional apparent diffusion coefficient changes investigated by diffusion-weighted spin-echo fMRI. Magn Reson Med 2006;56(6):1283–92.
[64] Song AW, Harshbarger T, Li T, Kim KH, Ugurbil K, Mori S, et al. Functional activation using apparent diffusion coefficient-dependent contrast allows better spatial localization to the neuronal activity: evidence using diffusion tensor imaging and fiber tracking. NeuroImage 2003;20(2):955–61.
[65] Darquie A, Poline JB, Poupon C, Saint-Jalmes H, Le Bihan D. Transient decrease in water diffusion observed in human occipital cortex during visual stimulation. Proc Natl Acad Sci U S A 2001;98 (16):9391–5.
[66] Le Bihan D, Urayama S, Aso T, Hanakawa T, Fukuyama H. Direct and fast detection of neuronal activation in the human brain with diffusion MRI. Proc Natl Acad Sci U S A 2006;103(21):8263–8.
[67] Le Bihan D. The 'wet mind': water and functional neuroimaging. Phys Med Biol 2007;52(7):R57–90.
[68] Kohno S, Sawamoto N, Urayama S, Aso T, Aso K, Seiyama A, et al. Water-diffusion slowdown in the human visual cortex on visual stimulation precedes vascular responses. J Cereb Blood Flow Metab 2009;29(6):1197–207.
[69] Yacoub E, Uludag K, Ugurbil K, Harel N. Decreases in ADC observed in tissue areas during activation in the cat visual cortex at 9.4 T using high diffusion sensitization. Magn Reson Imaging 2008; 26(7):889–96.
[70] Li T, Song AW. Fast functional brain signal changes detected by diffusion weighted fMRI. Magn Reson Imaging 2003;21(8):829–33.
[71] Jin T, Kim SG. Functional changes of apparent diffusion coefficient during visual stimulation investigated by diffusion-weighted gradient-echo fMRI. NeuroImage 2008;41(3):801–12.
[72] Miller KL, Bulte DP, Devlin H, Robson MD, Wise RG, Woolrich MW, et al. Evidence for a vascular contribution to diffusion FMRI at high b value. Proc Natl Acad Sci U S A 2007;104(52):20967–72.
[73] Risher WC, Andrew RD, Kirov SA. Real-time passive volume responses of astrocytes to acute osmotic and ischemic stress in cortical slices and in vivo revealed by two-photon microscopy. Glia 2009;57 (2):207–21.
[74] Brooks JC, Beckmann CF, Miller KL, Wise RG, Porro CA, Tracey I, et al. Physiological noise modelling for spinal functional magnetic resonance imaging studies. NeuroImage 2008;39(2):680–92.
[75] Figley CR, Stroman PW. Development and validation of retrospective spinal cord motion time-course estimates (RESPITE) for spin-echo spinal fMRI: improved sensitivity and specificity by means of a motion-compensating general linear model analysis. NeuroImage 2009;44(2):421–7.
[76] Glover GH, Li TQ, Ress D. Image-based method for retrospective correction of physiological motion effects in fMRI: RETROICOR. Magn Reson Med 2000;44(1):162–7.
[77] Poser BA, Norris DG. Fast spin echo sequences for BOLD functional MRI. MAGMA 2007;20(1):11–7.
[78] Ye Y, Zhuo Y, Xue R, Zhou XJ. BOLD fMRI using a modified HASTE sequence. NeuroImage 2010;49(1):457–66.
[79] Hoult DI, Chen CN, Sank VJ. The field dependence of NMR imaging: II. Arguments concerning an optimal field strength. Magn Reson Med 1986;3(5):730–46.
[80] Chen CN, Sank VJ, Cohen SM, Hoult DI. The field dependence of NMR imaging: I. Laboratory assessment of signal-to-noise ratio and power deposition. Magn Reson Med 1986;3(5):722–9.
[81] Bloombergen N, Purcell EM, Pound RV. Relaxation effects in nuclear magnetic resonance absorption. Phys Rev 1948;73:679–712.
[82] Yang P, Wang J, Chao Y. Functional magnetic resonance imaging at 0.35 T using SEEP contrast. Chinese Journal of Magnetic Resonance 2009;26(2):247–54.
[83] Cohen-Adad J, Gauthier C, Brooks JCW, Leblond H, Hoge RD, Fisher J, et al. Venous effect in spinal cord fMRI: insights from intrinsic optical imaging and laser speckle. NeuroImage 2009;47 (Supplement 1):S186.
[84] Golay X, Pruessmann KP, Weiger M, Crelier GR, Folkers PJ, Kollias SS, et al. PRESTO-SENSE: an ultrafast whole-brain fMRI technique. Magn Reson Med 2000;43(6):779–86.
[85] Josephs O, Turner R, Friston KJ. Event-related fMRI. Hum Brain Mapp 1997:5243–8.
[86] Buckner RL, Bandettini PA, O'Craven KM, Savoy RL, Petersen SE, Raichle ME, et al. Detection of cortical activation during averaged single trials of a cognitive task using functional magnetic resonance imaging. Proc Natl Acad Sci U S A 1996;93(25):14878–83.
[87] Dale AM. Optimal experimental design for event-related fMRI. Hum Brain Mapp 1999;8(2-3):109–14.